

# Defect complexes in Ti-doped sapphire: A first principles study.

L. Yu. Kravchenko<sup>1</sup>, D. V. Fil<sup>1,2\*</sup>

<sup>1</sup>*Institute for Single Crystals, National Academy of Sciences of Ukraine, 60 Nauky Avenue, Kharkiv 61001, Ukraine*

<sup>2</sup>*V.N. Karazin Kharkiv National University, 4 Svobody Square, Kharkiv 61022, Ukraine*

First-principles calculations have been performed to study the formation of defect complexes in Ti doped  $\alpha$ -Al<sub>2</sub>O<sub>3</sub> crystals. The formation energies of isolated Ti<sup>3+</sup> and Ti<sup>4+</sup> defects, pairs, triples and quadruples of Ti ions and Al vacancies are computed under different equilibrium conditions of Al-Ti-O related phases. Taking into account charge neutrality of the whole system we determine the equilibrium concentrations of simple and complex defects as well as the total equilibrium concentration of Ti in an  $\alpha$ -Al<sub>2</sub>O<sub>3</sub> crystal. It is shown that the equilibrium concentration of complex defects can be on the same order of or even larger than the concentrations of isolated substitutional Ti<sup>3+</sup> and Ti<sup>4+</sup> defects. It is found that in Ti-deficient conditions the relative fraction of isolated defects increases and the balance is shifted towards Ti<sup>4+</sup> defects. A universal relation between equilibrium concentrations of isolated and complex defects is obtained. The band structure of the system with complex defects is calculated and extra levels inside the band gap caused by such defects are found.

## I. INTRODUCTION

Doping of synthetic crystals with different activating ions provides desired optical and lasing properties of such materials [1]. Activating ions can be in different charge states, may occupy different crystallographic positions and form complexes of two or more impurity atoms situated close to each other or complexes of impurity atoms with intrinsic defects.

In particular, such a situation is realized in Ti:sapphire in which Ti ions can exist in different charge states and may form pairs, triples and multisite clusters. Ti: $\alpha$ -Al<sub>2</sub>O<sub>3</sub> is known as a laser material [2–6]. The laser efficiency of Ti:sapphire is affected by a residual infrared absorption in the emission band of the Ti:Al<sub>2</sub>O<sub>3</sub> laser. Crystal field calculations [7] support a hypothesis [5] that the absorption is caused by Ti<sup>3+</sup> – Ti<sup>4+</sup> pairs. The ratio of the absorption coefficients at the pump wavelength ( $\lambda = 514$  nm) and at the maximum of residual absorption ( $\lambda = 800$  nm) is known as the figure of merit (FoM) of Ti:sapphire laser crystals. FoM can be used to evaluate experimentally the concentration of Ti<sup>4+</sup> ions [8]. The Ti<sup>4+</sup> concentration can also be obtained from ultraviolet absorption spectra [9].

Defect formation energies and relative stability of defects in different charge states can be determined from the first-principles calculations. The formation energy depends on the oxygen chemical potential  $\mu_O$  and the electron Fermi energy  $E_F$ . In [10] the formation energies of intrinsic (native) defects in pure  $\alpha$ -Al<sub>2</sub>O<sub>3</sub> were obtained using the plane-wave pseudopotential method. Considering various charge states of the defects, the authors of [10] found that the defect species in their highest charge state exhibit the smallest formation energies. According to [10], in a wide range of  $\mu_O$  the formation energies of charged vacancies ( $V$ ) and interstitial ions ( $i$ ) are in the order of  $V_{Al}^{3-} < O_i^{2-} < V_O^{2+} < Al_i^{3+}$ . The

formation energies of Schottky and Frenkel defects were also calculated in [10]. These energies are independent of  $\mu_O$ . It was found that the Schottky quintet has the formation energy per defect smaller than O Frenkel and Al Frenkel pairs have. In addition, the formation energy of Al Frenkel pairs is smaller than that of O Frenkel pairs.

The dependence of the formation energies of native defects in  $\alpha$ -Al<sub>2</sub>O<sub>3</sub> on  $\mu_O$  and  $E_F$  was found in [11]. It was shown that over most of the range of  $E_F$  the defects in their highest charge states dominate. Nevertheless a significant amount of defects in lower charge states can emerge at some  $\mu_O$  and  $E_F$ . In particular, the formation energy of the oxygen vacancy  $V_O^{1+}$  can be comparable to the energy of other defects. This result correlates with the experimental observation of F<sup>+</sup> centers in  $\alpha$ -Al<sub>2</sub>O<sub>3</sub> [12]. Calculations [11] support the conclusion of [10] that for the charge neutral combinations the formation energy ordering is Schottky < Al Frenkel < O Frenkel.

The charge states and formation energies of vacancies, interstitial and antisite atoms in pure  $\alpha$ -Al<sub>2</sub>O<sub>3</sub> were studied in [13]. It was found that under O-rich and O-deficient conditions the most stable defect is the Al vacancy  $V_{Al}^{3-}$ . According to [13] the preferable charge state of O vacancies is  $V_O^0$ . In O-rich conditions the formation energies are ordered as  $V_{Al}^{3-} < O_{Al}^{3-} < O_i^{2-} < V_O^0 < Al_i^{3+} < Al_O^{3+}$ , and in O-deficient conditions, as  $V_{Al}^{3-} < O_i^{2-} < Al_i^{3+} < O_{Al}^{3-} < V_O^0 < Al_O^{3+}$ , where O<sub>Al</sub> and Al<sub>O</sub> correspond to O and Al antisite atoms, respectively. The energy ordering for neutral combinations of native defects is Schottky defect < cation Frenkel < anion Frenkel < antisite pair. The charge states of the components of the most stable Schottky and Frenkel defects in [13] differ from one obtained in [10, 11].

In [14] the energetics of point defects in Ti-doped Al<sub>2</sub>O<sub>3</sub> was studied. Substitutional and interstitial Ti ions with charge compensating intrinsic defects were considered and their formation energies against the oxygen chemical potential were calculated. It was found that substitutional Ti<sup>4+</sup> ions with charge compensating Al vacancies are the most stable defects in the oxidized con-

\* fil@isc.kharkov.ua

ditions. In contrast, the formation energy of substitutional  $\text{Ti}^{3+}$  ions is minimal in the reduced conditions. In the intermediate range of the oxygen potential the substitutional  $\text{Ti}^{3+}$  and  $\text{Ti}^{4+}$  ions exhibit similar formation energies.

In [15] the formation of Ti clusters in Ti-doped  $\text{Al}_2\text{O}_3$  was investigated. It was shown that  $\text{Ti}^{3+}$  clusters have a positive binding energy. The binding energy increases with decreasing the distance between  $\text{Ti}^{3+}$  ions and with increasing the number of ions in the cluster. It was also found that the binding energy of a complex of a substitutional  $\text{Ti}^{4+}$  ion and an Al vacancy  $V_{\text{Al}}^{3-}$  is rather large.

In this paper we calculate equilibrium concentrations of isolated and complex defects in Ti-doped  $\alpha\text{-Al}_2\text{O}_3$ . A positive binding energy does not automatically mean that all isolated defects bind in clusters. The equilibrium concentrations of defects correspond to the minimum of free energy. The free energy contains the entropy term and the clustering results in lowering of entropy. In the general case both the complex and isolated defects are present. We find that the equilibrium concentration of a given complex defect specie is proportional to the product of the equilibrium concentrations of simple defects which form the complex defect. The coefficient of proportionality is determined by the binding energy and the temperature. The first principles calculations show that the concentration of  $\text{Ti}^{3+} - \text{Ti}^{3+}$  pairs can be on the same order of or even larger than the concentration of isolated  $\text{Ti}^{3+}$ , while the relative amount of  $\text{Ti}^{3+} - \text{Ti}^{3+} - \text{Ti}^{3+}$  triples is small over the entire range of allowed  $\mu_{\text{O}}$ .

The minimum of free energy of the system with charged defects should be found under the additional condition that the overall charge of the defects is equal to zero. It is dictated by charge neutrality of the system. We do not consider any particular charge compensating defects. Charge neutrality requires that all negatively charged defects compensate all positively charged defects or vice versa. Applying this condition we find that the equilibrium concentrations of charged defects are determined by the formation energies of electrically neutral combinations of charged defects. These combinations can be chosen in an arbitrary way. The formation energies for electrically neutral combinations of defects do not depend on the Fermi energy. Therefore, the equilibrium concentrations of charged defects are independent of  $E_F$  irrespectively to the dependence of their formation energies on  $E_F$ . We obtain that in addition to  $\text{Ti}^{4+}$  isolated defects a great amount of  $\text{Ti}^{4+} - V_{\text{Al}}^{3-}$  pairs,  $\text{Ti}^{4+} - V_{\text{Al}}^{3-} - \text{Ti}^{4+}$  triples and  $\text{Ti}^{4+} - \text{Ti}^{4+} - \text{Ti}^{4+} - V_{\text{Al}}^{3-}$  quadruples emerge. The maximum concentration of  $\text{Ti}^{3+} - \text{Ti}^{4+}$  pairs is reached at intermediate values of the oxygen chemical potential and over the entire range of  $\mu_{\text{O}}$  this concentration is smaller than the concentration of isolated  $\text{Ti}^{3+}$  defects.

It is shown that the ratio of the concentrations of different defect species is changed in Ti-deficient conditions. At such conditions most of Ti ions enter into the crystal in the form of isolated  $\text{Ti}^{3+}$  and  $\text{Ti}^{4+}$  substitutional de-

fects, and the balance between  $\text{Ti}^{3+}$  and  $\text{Ti}^{4+}$  is shifted towards  $\text{Ti}^{4+}$ .

The band structure of the system with isolated and complex Ti defects is calculated. It is found that the clustering of defects results in a shift of defects levels with respect to the valence band maximum and in splitting of the levels.

## II. METHOD AND COMPUTATIONAL DETAILS

Calculations were performed by the pseudopotential method with the use of a strictly localized atom-centered basis set as implemented in the open source SIESTA code [16] based on the density-functional theory (DFT) approach. The pseudopotentials were generated with the improved Troullier-Martins scheme. The O –  $2s^22p^4$ , Al –  $3s^23p^1$  and Ti –  $4s^13d^3$  electron states were considered as valence configurations and a small core correction was applied. The generalized gradients approximation with the Perdew-Burke-Ernzerhof (PBE) exchange-correlation functional and the double-zeta basis set plus polarization orbitals was employed. Primitive translation vectors were allowed to relax until the maximum residual stress component converged to less than 0.1 GPa and atomic positions were optimized until the residual forces had been less than 0.01 eV/Å. A real-space grid with the plane-wave cutoff energy  $E_c = 250$  Ry was used to calculate the total energy of the system. Selective tests showed that the total energy was converged within 0.68 meV/atom for the total energies obtained at  $E_c = 300$  Ry. In view of large size of the supercell we performed numerical integration over the Brillouin zone only at the  $\Gamma$  point.

To calculate the formation energy of a given defect a supercell of four fully optimized unit cells ( $4 \times 30$  atoms) was built. One isolated or complex defect was placed in the supercell and the optimization of atomic positions was fulfilled again. The total energy was calculated for the optimized defect supercell.

The formation energy of a defect  $E_i$  is determined by the difference [17]

$$E_i = E_{def} - E_{perf} + n_{\text{Al}}\mu_{\text{Al}} + n_{\text{O}}\mu_{\text{O}} - n_{\text{Ti}}\mu_{\text{Ti}} + q_i E_F, \quad (1)$$

where  $E_{def}$  and  $E_{perf}$  are the total energies of the defect and perfect supercell, correspondingly,  $n_{\text{Al}}$  and  $n_{\text{O}}$  are the numbers of Al and O atoms removed from the perfect supercell,  $n_{\text{Ti}}$  is the number of Ti atoms added,  $\mu_{\text{Al}}$ ,  $\mu_{\text{O}}$  and  $\mu_{\text{Ti}}$  are the chemical potentials of Al, O and Ti, correspondingly, and  $q_i$  is the defect charge in elementary charge units.

The chemical potentials of Al and Ti vary depending on equilibrium conditions of a multiphase Al – Ti – O ternary system. To determine these conditions we calculated the formation energies of  $\alpha\text{-Al}_2\text{O}_3$ ,  $\text{TiO}_2$ ,  $\text{Ti}_2\text{O}_3$ ,  $\text{TiO}$ ,  $\text{Ti}_2\text{O}$ ,  $\text{TiAl}$ ,  $\text{TiAl}_2$  and  $\text{TiAl}_3$  crystals and built the Al – Ti – O phase diagram. Calculations were done by the same method with the same pseudopotentials as ones

TABLE I. Calculated and experimental lattice parameters (in Å) of materials used as reference ones for building the Al – Ti – O phase diagram.

Crystal	Space group	Lattice parameters (Theory)	Lattice parameters (Experiment)
Al	<i>Fm3m</i>	$a = 4.07$	$a = 4.05$ [18]
Al <sub>2</sub> O <sub>3</sub>	<i>R3c</i>	$a = 4.86, c = 13.19$	$a = 4.77, c = 13.00$ [19]
TiO <sub>2</sub>	<i>P4<sub>2</sub>/mnm</i>	$a = 4.69, c = 2.99$	$a = 4.59, c = 2.96$ [20]
Ti <sub>2</sub> O <sub>3</sub>	<i>R3c</i>	$a = 5.14, c = 14.10$	$a = 5.16, c = 13.61$ [21]
TiO	<i>C2/m</i>	$a = 5.87, b = 9.42$ $c = 4.22, \gamma = 107^\circ 13'$	$a = 5.86, b = 9.34,$ $c = 4.14, \gamma = 107^\circ 32'$ [22]
Ti <sub>2</sub> O	<i>P3m1</i>	$a = 3.01, c = 4.86$	$a = 2.92, c = 4.71$ [23]
TiAl	<i>P4/mmm</i>	$a = 2.84, c = 4.12$	$a = 2.83, c = 4.06$ [18]
TiAl <sub>2</sub>	<i>I4<sub>1</sub>/amd</i>	$a = 4.00, c = 24.45$	$a = 3.97, c = 24.31$ [24]
TiAl <sub>3</sub>	<i>I4/mmm</i>	$a = 3.87, c = 8.69$	$a = 3.84, c = 8.58$ [18]
Ti	<i>P6/mmm</i>	$a = 2.96, c = 4.66$	$a = 2.95, c = 4.68$ [18]

TABLE II. Calculated formation energies  $\Delta H_f$  per atom (in eV) for crystals listed in Table I.

Crystal	Al <sub>2</sub> O <sub>3</sub>	TiO <sub>2</sub>	Ti <sub>2</sub> O <sub>3</sub>	TiO	Ti <sub>2</sub> O	TiAl	TiAl <sub>2</sub>	TiAl <sub>3</sub>
$\Delta H_f$	-3.42	-3.42	-3.35	-2.92	-2.06	-0.45	-0.47	-0.44

used for the obtaining of the supercell energies  $E_{def}$  and  $E_{perf}$ . The formation energy for a crystal with the general formula  $Al_xTi_yO_z$  is given by the equation

$$\Delta H_f = \mu_{Al_xTi_yO_z} - x\mu_{Al} - y\mu_{Ti} - \frac{z}{2}\mu_{O_2}, \quad (2)$$

where  $\mu_{Al}$  and  $\mu_{Ti}$  are the energies per atom in the metallic phases,  $\mu_{O_2}$  is the internal energy of O<sub>2</sub> molecule. Lattice parameters obtained by structure optimization calculations are presented in Table I. For comparison, experimental lattice parameters are also given in Table I. The computed formation energies are given in Table II. The Al – Ti – O phase diagram obtained from the computed formation energies is shown in Fig. 1.

We consider the growth conditions in which the Al<sub>2</sub>O<sub>3</sub> phase is in equilibrium with two other phases. These conditions correspond to the points in the phase diagram specified in Table III. At the point A the chemical potentials of Al, Ti and O atoms are related by the equations

$$2\mu_{Al} + 3\mu_O = \mu_{Al_2O_3}, \quad (3)$$

$$\mu_{Ti} + 2\mu_O = \mu_{TiO_2}, \quad (4)$$

$$2\mu_O = \mu_{O_2}. \quad (5)$$

The right-hand parts of Eqs. (3)-(5) contain the energies (per formula unit) of the compounds which are in equilibrium at the point A. Solving (3)-(5) one gets the potentials  $\mu_{Al}$ ,  $\mu_O$  and  $\mu_{Ti}$ . Similar equations can be written for the points B, C etc. The oxygen potential  $\mu_O$  (see Table III) varies from the largest value at the point A that corresponds to the oxidized limit to the lowest value at the point F that corresponds to the reduced limit. The value of  $\mu_O$  given in Table III is counted from the chemical potential of an isolated oxygen atom.

TABLE III. Reference equilibrium points in the phase diagram Fig. 1.

Point label	Compounds in equilibrium with Al <sub>2</sub> O <sub>3</sub>	$\mu_O$ (in eV)
A	O <sub>2</sub> , TiO <sub>2</sub>	-4.39
B	TiO <sub>2</sub> , Ti <sub>2</sub> O <sub>3</sub>	-8.18
C	Ti <sub>2</sub> O <sub>3</sub> , TiO	-9.46
D	TiO, TiAl <sub>2</sub>	-9.77
E	TiAl <sub>2</sub> , TiAl <sub>3</sub>	-9.87
F	TiAl <sub>3</sub> , Al	-10.09

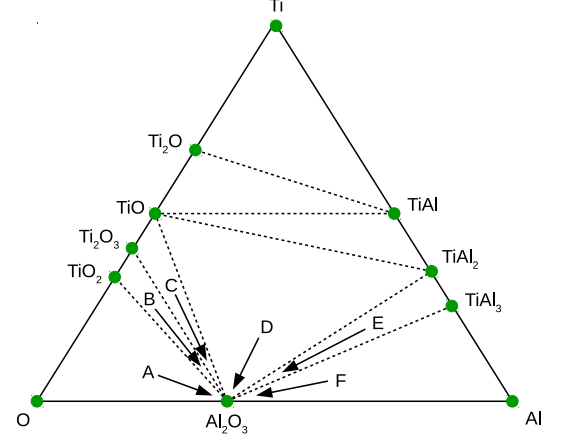


FIG. 1. Computed phase diagram of the Al-Ti-O ternary system. The points A - F denoted by arrows correspond to the vertices of the three-phase region around Al<sub>2</sub>O<sub>3</sub>.

### III. RESULTS AND DISCUSSIONS

#### A. Formation energies and binding energies

The formation energy of an electrically neutral defect (Eq. (1) with  $q_i = 0$ ) does not depend on the Fermi energy  $E_F$ . The contribution of such defects into the free energy and their equilibrium concentrations are independent of  $E_F$  as well. On the contrary, the formation energy of a charged defect (Eq. (1) with  $q_i \neq 0$ ) depends on  $E_F$ . One can exclude  $E_F$  from the problem considering electrically neutral combinations of charged defects. The formation energy of any neutral combination is independent of  $E_F$ . Taking into account overall charge neutrality of the crystal one finds that the equilibrium concentrations of charged defects are independent of  $E_F$  as well. To compute these concentrations one should know only the formation energies of electrically neutral combinations of charged defects.

Electrically neutral combinations can be chosen in an arbitrary way and a concrete choice is just the matter of convention. The result of calculations of the equilibrium concentrations will be the same for any choice. Here we consider positively charged defects in a combination

with negatively charged  $V_{\text{Al}}^{3-}$  vacancies, and negatively charged defects, in a combination with positively charged  $\text{Ti}^{4+}$  substitutional defects.

We restrict the analysis with complex defects formed by substitutional  $\text{Ti}_{\text{Al}}^{3+}$  and  $\text{Ti}_{\text{Al}}^{4+}$  ions, and  $V_{\text{Al}}^{3-}$  vacancies. Below we use the notations  $\text{Ti}^{3+}$  and  $\text{Ti}^{4+}$  for  $\text{Ti}_{\text{Al}}$  substitutional defects. For completeness we also take into account isolated interstitial ions (notated as  $\text{Ti}_i^{3+}$  and  $\text{Ti}_i^{4+}$ ), and intrinsic defects  $V_{\text{O}}^{2+}$ ,  $\text{Al}_i^{3+}$  and  $\text{O}_i^{2-}$ . Intrinsic defects are considered in electrically neutral combinations that correspond to the Schottky quintet ( $3V_{\text{O}}^{2+}, 2V_{\text{Al}}^{3-}$ ), Al Frenkel ( $\text{Al}_i^{3+}, V_{\text{Al}}^{3-}$ ) pair and O Frenkel ( $\text{O}_i^{2-}, V_{\text{O}}^{2+}$ ) pair.

For each defect specie we compute the energy of the supercell with one isolated or complex defect. A charge state of the defect is set as a charge of the whole supercell. The formation energy of an electrically neutral combination of defects  $\tilde{E}_\lambda$  is defined as the sum of the formation energies (1) calculated for the corresponding supercells and divided by the number of the supercells. The quantity  $\tilde{E}_\lambda$  yields the formation energy per defect and  $\lambda$  stands for a given electrically neutral combination.

We will show below that the concentration of complex defects can be expressed through their binding energy. The binding energy of a complex defect formed by  $x$   $\text{Ti}^{3+}$ ,  $y$   $\text{Ti}^{4+}$  and  $z$   $V_{\text{Al}}^{3-}$  vacancies is defined as

$$E_i^{(b)} = xE_3 + yE_4 + zE_V - E_i, \quad (6)$$

where  $E_3$ ,  $E_4$  and  $E_V$  are the formation energies (1) of isolated  $\text{Ti}^{3+}$ ,  $\text{Ti}^{4+}$  and  $V_{\text{Al}}^{3-}$  defects, correspondingly. Substituting Eq. (1) into the right-hand part of Eq. (6) we find that the chemical potentials  $\mu_{\text{Al}}$ ,  $\mu_{\text{O}}$  and  $\mu_{\text{Ti}}$  are canceled. Therefore, the binding energy is the same at different points of the ternary phase diagram Fig. 1. The binding energy can be expressed through the formation energies of electrically neutral defects and the formation energies of electrically neutral combinations of charged defects taken at the same equilibrium point.

The formation energy of a complex defect and its binding energy depends on the distances between simple defects which form the complex defect. In  $\alpha\text{-Al}_2\text{O}_3$  every Al atom has four nearest neighbor Al sites. These four sites form a tetrahedron (Fig. 2). The distances between a given Al site and four nearest neighbor Al sites are almost the same (the link along the  $[0001]$  axis is shorter by 0.14 Å). We consider pairs where substitutional ions and Al vacancies are located at two nearest neighbor sites (the central site and a tetrahedron apex shown in Fig. 2). Four different orientations of such pairs are possible. We obtain the same binding energy for three orientations and a slightly different binding energy (the difference is about or less than 0.1 eV) for the fourth orientation (that corresponds to the shortest link). We neglect this difference under the obtaining of the equilibrium concentrations of the defects. Triple defects under study are formed by single defects located at the central site and at two tetrahedron apexes. We account two types of  $\text{Ti} - \text{Ti} - V$

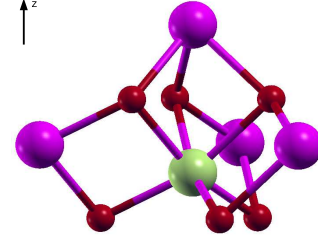


FIG. 2. Locations of four nearest neighbor Al atoms (large purple circles) around a given (central) Al site (large green circle). Nearest neighbor O sites are shown by small red circles. The direction of the shortest Al – Al link is shown by the arrow.

TABLE IV. Computed binding energies of complex defects (in eV).

Complex defect	$E^{(b)}$
$\text{Ti}^{3+} - \text{Ti}^{3+}$	1.36
$\text{Ti}^{3+} - \text{Ti}^{4+}$	0.70
$\text{Ti}^{4+} - \text{Ti}^{4+}$	-0.11
$\text{Ti}^{3+} - V_{\text{Al}}^{3-}$	0.30
$\text{Ti}^{4+} - V_{\text{Al}}^{3-}$	1.15
$V_{\text{Al}}^{3-} - V_{\text{Al}}^{3-}$	-3.25
$\text{Ti}^{3+} - \text{Ti}^{4+} - V_{\text{Al}}^{3-}$	1.91
$\text{Ti}^{3+} - V_{\text{Al}}^{3-} - \text{Ti}^{4+}$	2.05
$\text{Ti}^{4+} - \text{Ti}^{4+} - V_{\text{Al}}^{3-}$	1.30
$\text{Ti}^{4+} - V_{\text{Al}}^{3-} - \text{Ti}^{4+}$	2.15
$\text{Ti}^{3+} - \text{Ti}^{3+} - V_{\text{Al}}^{3-}$	2.16
$\text{Ti}^{3+} - V_{\text{Al}}^{3-} - \text{Ti}^{3+}$	1.19
$\text{Ti}^{3+} - \text{Ti}^{3+} - \text{Ti}^{3+}$	2.03
$\text{Ti}^{4+} - \text{Ti}^{4+} - \text{Ti}^{4+} - V_{\text{Al}}^{3-}$	2.93

complexes, one is with a Ti ion at the central site and the other is with an Al vacancy at the central site. For the latter we use the notation  $\text{Ti} - V - \text{Ti}$ . Triple defects can be in 6 different orientations. We consider one quadruple defect specie. The quadruple defect is formed by a  $V_{\text{Al}}^{3-}$  vacancy located at the central site surrounded with three nearest neighbor substitutional Ti ions.

The binding energies are given in Table IV. One can see that all binding energies except ones of  $\text{Ti}^{4+} - \text{Ti}^{4+}$  and  $V_{\text{Al}}^{3-} - V_{\text{Al}}^{3-}$  pairs are positive. Negative binding energy corresponds to the repulsion. Below we do not consider complex defects with negative binding energy.

The computed formation energies of electrically neutral defects and of electrically neutral combinations of charged defects are presented in Fig. 3. The energies that correspond to energetically preferable orientations (configurations) of complex defects are displayed.



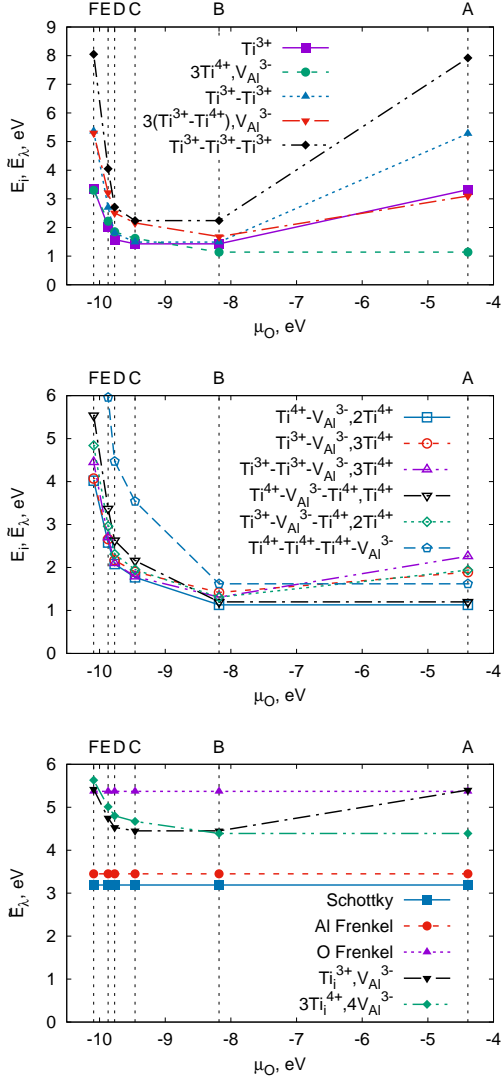


FIG. 3. Formation energies per defect of electrically neutral defects ( $E_i$ ) and electrically neutral combinations of charged defects ( $\tilde{E}_\lambda$ ) at the equilibrium points A - F. Lines are guides to the eye. The value of the oxygen chemical potential is shown in the abscissa axis.

### B. Equilibrium concentrations of defects

The free energy of defects in a crystal is given by the defect formation energies  $E_i$ , the defect numbers  $n_i$ , and the configurational entropy (the logarithm of the number of ways  $W_i$  to place  $n_i$  defects in a crystal):

$$F = \sum_i (E_i n_i - k_B T \ln W_i), \quad (7)$$

where  $k_B$  is the Boltzmann constant, and  $T$  is the temperature. Since usually the total number of sites is much larger than the defect numbers each defect specie can be

considered independently. Then

$$W_i = \frac{N_i!}{(N_i - n_i)! n_i!}, \quad (8)$$

where  $N_i$  is the number of ways to place one defect of a given specie into a crystal. Below we imply  $N_i \gg n_i \gg 1$ .

For isolated substitutional Ti defects and Al vacancies the quantity  $N_i$  is the number of Al atoms in the perfect crystal:  $N_i = N_{\text{Al}}$ . For complex defects the quantity  $N_i$  accounts also different equivalent orientations of defects. It can be expressed as  $N_i = a_i N_{\text{Al}}$ , where  $a_i$  is a factor that depends on the defect type. It is equal to  $a_i = 2$  for Ti-Ti pairs,  $a_i = 4$  for Ti-V pairs and Ti-Ti-Ti-V quadruples, and  $a_i = 6$  for the triples. For  $\text{Ti}_i$  the factor  $a_i = 1/2$  is the ratio of the number of empty O octahedral interstices to  $N_{\text{Al}}$ .

The defect numbers  $n_i$  are found from the condition of minimum of the free energy. For neutral defect species the extremum condition yields

$$\tilde{n}_i = \frac{n_i}{N_i} = \exp\left(-\frac{E_i}{k_B T}\right). \quad (9)$$

The additional constraint for charged defects is  $\sum_i q_i n_i = 0$ , where  $q_i$  is a defect charge in units of elementary charge. It is convenient to separate the contribution of  $\text{Ti}^{4+}$  ( $n_4$ ) and  $V_{\text{Al}}^{3-}$  ( $n_V$ ) in the charge neutrality constraint:

$$n_4 - 3n_V + \sum_{i \neq 4, V} q_i n_i = 0. \quad (10)$$

Then, we exclude  $n_V$  from the free energy (7) and obtain the extremum conditions for the energy (7) with respect to  $n_4$  and all other  $n_i$ :

$$E_4 + \frac{1}{3}E_V + k_B T \left( \ln \tilde{n}_4 + \frac{1}{3} \ln \tilde{n}_V \right) = 0, \quad (11)$$

$$\frac{q_i}{3}E_V + E_i + k_B T \left( \frac{q_i}{3} \ln \tilde{n}_V + \ln \tilde{n}_i \right) = 0, \quad (12)$$

where  $\tilde{n}_i = n_i/N_i$ . One finds from Eqs. (11) and (12) the relations

$$\tilde{n}_4^3 \tilde{n}_V = \exp\left(-\frac{4\tilde{E}_{4,V}}{k_B T}\right), \quad (13)$$

$$\tilde{n}_i = \tilde{n}_4^{q_i} \exp\left(-\frac{E_i - q_i E_4}{k_B T}\right), \quad (i \neq 4, V), \quad (14)$$

where  $\tilde{E}_{4,V} = (3E_4 + E_V)/4$  is the formation energy per defect of a combination of three  $\text{Ti}^{4+}$  and one  $V_{\text{Al}}^{3-}$ . We note that Eq. (14) describes the case of neutral defects as well (at  $q_i = 0$  it reduces to Eq. (9)).

One can easily check that the energies  $E_i - q_i E_4$  in Eq. (14) are expressed through the formation energies  $\tilde{E}_\lambda$ . Respectively, the equilibrium concentrations are determined by  $\tilde{E}_\lambda$  and do not depend on  $E_F$ . Substituting Eq. (14) into Eqs. (10) and taking (13) we have

two algebraical equations for the variables  $\tilde{n}_4$  and  $\tilde{n}_V$ . These equations have a unique positive real-valued solution. From this solution and Eq. (14) we obtain the concentrations of all considered defect species.

Eqs. (13) and (14) allow us to express the concentrations of complex defects through the concentrations of isolated defects. The equilibrium concentration of complex defects composed of  $r_3$   $\text{Ti}^{3+}$  ions,  $r_4$   $\text{Ti}^{4+}$  ions and  $r_V$   $V_{\text{Al}}^{3-}$  vacancies is equal to

$$\tilde{n}_i = (\tilde{n}_3)^{r_3} (\tilde{n}_4)^{r_4} (\tilde{n}_V)^{r_V} \exp\left(\frac{E_i^{(b)}}{k_B T}\right), \quad (15)$$

where  $E_i^{(b)}$  is the binding energy (6). Eq. (15) can be applied instead of Eq. (14) to calculate equilibrium concentrations of complex defects. Eq. (15) can be also useful if the concentrations of isolated defects are known, for instance, from experimental data.

In the charge neutrality equation (10) it is enough to take into account  $\text{Ti}^{4+}$  and  $V_{\text{Al}}^{3-}$  isolated defects, and some other defect species with the smallest formation energies. Then solving the obtained system for  $\tilde{n}_4$  and  $\tilde{n}_V$  and substituting the answer into Eq. (14) or Eq. (15) one finds the concentrations of the rest defect species. Such an approximation is valid if the overall concentration of species neglected in the charge neutrality equation is small in comparison with the concentration of species accounted in it. Relative error in determining the concentrations is proportional to that small parameter.

Below we exclude the point F from the consideration and account  $\text{Ti}^{4+}$ ,  $V_{\text{Al}}^{3-}$ ,  $\text{Ti}^{4+} - V_{\text{Al}}^{3-}$  and  $\text{Ti}^{4+} - V_{\text{Al}}^{3-} - \text{Ti}^{4+}$  defects in the charge neutrality equation. Using Eq. (15) we obtain

$$\tilde{n}_4 - 3\tilde{n}_V - 8\tilde{n}_4\tilde{n}_V e^{\frac{E_{4V}^{(b)}}{k_B T}} - 6\tilde{n}_4^2\tilde{n}_V e^{\frac{E_{4V4}^{(b)}}{k_B T}} = 0, \quad (16)$$

where  $E_{4V}^{(b)}$  and  $E_{4V4}^{(b)}$  are the binding energies of  $\text{Ti}^{4+} - V_{\text{Al}}^{3-}$  pairs and  $\text{Ti}^{4+} - V_{\text{Al}}^{3-} - \text{Ti}^{4+}$  triples, correspondingly. The solution of Eqs. (13) and (16) can be presented in the form

$$\tilde{n}_4 = z\tilde{n}_4^{(0)}, \quad (17)$$

where  $\tilde{n}_4^{(0)} = 3^{1/4} \exp(-\tilde{E}_{4,V}/k_B T)$  is the approximate solution obtained under accounting of only  $\text{Ti}^{4+}$  and  $V_{\text{Al}}^{3-}$  in the charge neutrality equation (16). The factor  $z$  satisfies the equation

$$z^4 - \alpha z - \beta z^2 = 1. \quad (18)$$

The coefficients  $\alpha$  and  $\beta$  in Eq. (18) are equal to

$$\alpha = \frac{8}{3^{3/4}} e^{-\frac{3(\tilde{E}_{4V4} - \tilde{E}_{4,V})}{k_B T}}, \quad (19)$$

$$\beta = \frac{6}{\sqrt{3}} e^{-\frac{2(\tilde{E}_{4V4,4} - \tilde{E}_{4,V})}{k_B T}}, \quad (20)$$

where  $\tilde{E}_{4V,4}$  and  $\tilde{E}_{4V4,4}$  are the formation energies (per defect) of the corresponding electrically neutral combinations (one  $\text{Ti}^{4+} - V_{\text{Al}}^{3-}$  pair plus two isolated  $\text{Ti}^{4+}$  and one  $\text{Ti}^{4+} - V_{\text{Al}}^{3-} - \text{Ti}^{4+}$  triple plus one isolated  $\text{Ti}^{4+}$ , respectively).

The factor  $z$  is defined as a positive real-valued root of Eq. (18). For  $\tilde{E}_{4V,4} - \tilde{E}_{4,V} \gg k_B T$  and  $\tilde{E}_{4V4,4} - \tilde{E}_{4,V} \gg k_B T$  the coefficients  $\alpha$  and  $\beta$  approach zero and  $\tilde{n}_4$  coincides with  $\tilde{n}_4^{(0)}$ .

The concentrations of other charged defects are calculated from Eq. (14). Substituting Eq. (17) into Eq. (14) we find that these quantities are expressed through the formation energies  $\tilde{E}_\lambda$ . In particular, for positively charged defects ( $q_i > 0$ )

$$\tilde{n}_i \approx \tilde{n}_4 (\sqrt[4]{3}z)^{q_i-1} e^{-(1+\frac{q_i}{3})\frac{\tilde{E}_{i,V} - \tilde{E}_{4,V}}{k_B T}}, \quad (21)$$

where the index  $\lambda = i, V$  stands for a combination of three positively charged defects and  $q_i$   $V_{\text{Al}}^{3-}$  vacancies. For negatively charged defects ( $q_i < 0$ )

$$\tilde{n}_i \approx \frac{\tilde{n}_4}{(\sqrt[4]{3}z)^{1+|q_i|}} e^{-(1+|q_i|)\frac{\tilde{E}_{i,4} - \tilde{E}_{4,V}}{k_B T}}, \quad (22)$$

where  $\lambda = i, 4$  stands for a combination of one negatively charged defect and  $|q_i|$  substitutional  $\text{Ti}^{4+}$ .

The concentrations of intrinsic defects obtained in a similar way are equal to

$$\tilde{n}_{V_{\text{Al}}^{3-}} \approx \frac{\tilde{n}_4}{3z^4}, \quad (23)$$

$$\tilde{n}_{\text{O}^{2+}} \approx \tilde{n}_4 \sqrt[4]{3}z e^{-\frac{5}{3}\frac{\tilde{E}_{\text{Sch}} - \tilde{E}_{4,V}}{k_B T}}, \quad (24)$$

$$\tilde{n}_{\text{Al}_i^{3+}} \approx \tilde{n}_4 (\sqrt[4]{3}z)^2 e^{-\frac{2(\tilde{E}_{\text{Al Frenkel}} - \tilde{E}_{4,V})}{k_B T}}, \quad (25)$$

$$\tilde{n}_{\text{O}_i^{2-}} \approx \frac{\tilde{n}_4}{(\sqrt[4]{3}z)^3} e^{-\frac{2\tilde{E}_{\text{O Frenkel}} - \frac{5}{3}\tilde{E}_{\text{Sch}} - \frac{1}{3}\tilde{E}_{4,V}}{k_B T}}, \quad (26)$$

where  $\tilde{E}_{\text{Frenkel Al(O)}}$  and  $\tilde{E}_{\text{Sch}}$  are the formation energies per one defect site for O(Al) Frenkel pair and for the Schottky quintet, respectively. Note that Eqs. (24)-(26) are applicable if the concentrations of the corresponding defects are small compared to the concentration of substitutional  $\text{Ti}^{4+}$  ions. The latter is provided by the smallness of the formation energy  $\tilde{E}_{4,V}$  in comparison with the Schottky and Frenkel defect formation energies. We emphasize that Eqs. (23)-(26) cannot be applied to pure  $\text{Al}_2\text{O}_3$ . Considering pure crystals one should account only intrinsic defects in the charge neutrality equation. It results in different from (23)-(26) equilibrium concentrations.

It is instructive to find distribution of Ti impurities between different defect species. The partial concentration of Ti that corresponds to the  $i$ -th defect specie is given by the expression

$$w_i = \tilde{n}_i a_i k_i \frac{2m_{\text{Ti}}}{m_{\text{Al}_2\text{O}_3}} \cdot 100\%, \quad (27)$$

where  $m_{\text{Ti}}$  and  $m_{\text{Al}_2\text{O}_3}$  are the molecular masses of Ti and  $\text{Al}_2\text{O}_3$ ,  $k_i$  is the number of Ti atoms in a given defect and  $a_i$  is the orientation factor defined above. The quantities  $w_i$  are the partial concentrations in percent by mass (wt%). Calculated  $w_i$  at the temperature  $T = 1600$  K are shown in Fig. 4. The sum  $w_{\text{Ti}} = \sum_i w_i$  yields the total equilibrium concentration of Ti. This quantity is also shown in Fig. 4. One finds from Fig. 4 that the overall concentration of charged defects neglected in Eq. (16) is about or less than one hundredth of  $\text{Ti}^{4+}$  concentration. The concentrations of  $\text{Ti}_i^{3+}$  and  $\text{Ti}_i^{4+}$  interstitial defects are too small and out of range of  $w_i$  in Fig. 4.

One can see from Fig. 4 that in the oxidized limit (point A) Ti is mainly in the form of isolated substitutional  $\text{Ti}^{4+}$  ions, while in the reduced limit (point E) it is in the form of isolated substitutional  $\text{Ti}^{3+}$ . In the oxidized (point A) and intermediate (point B) conditions a noticeable part of  $\text{Ti}^{4+}$  ions form pairs, triples or quadruples with  $V_{\text{Al}}^{3-}$  vacancies. In the intermediate conditions (points B and C) most of  $\text{Ti}^{3+}$  ions bind in  $\text{Ti}^{3+} - \text{Ti}^{3+}$  pairs. The concentration of  $\text{Ti}^{3+} - \text{Ti}^{4+}$  pairs reaches its maximum in the intermediate conditions (point B), but it remains much smaller than the concentration of isolated  $\text{Ti}^{3+}$ . At the point B most of  $\text{Ti}^{3+} - \text{Ti}^{4+}$  pairs bind in triples with  $V_{\text{Al}}^{3-}$  vacancies. The largest relative concentration (about  $10^{-2}$  of the total Ti concentration) of triples  $\text{Ti}^{3+} - \text{Ti}^{3+} - \text{Ti}^{3+}$  is reached at the point C. Over the entire range of  $\mu_{\text{O}}$  the amount of Ti distributed between other defects is smaller than  $10^{-2}$  of the total Ti amount.

The computed concentrations of intrinsic defects are shown in Fig. 5. One can see that the concentrations of native defects excluding  $V_{\text{Al}}^{3-}$  are rather small, and therefore one can omit their contribution into the charge neutrality equation (10).

The results presented in Figs. 4 and 5 have been obtained neglecting temperature effects on the chemical potential of the precursors. It is connected with that DFT is the zero-temperature technique. It was proposed in [25, 26] to account temperature effects within the approach that combines DFT and classical thermodynamics. In [25, 26] the approach was used for the obtaining of  $(T, p)$  phase diagrams of surface structures. Similar approach was implemented in [11] for the calculation of the formation energies of native defects in  $\text{Al}_2\text{O}_3$ . Below we account temperature corrections to the defect formation energies in Ti-doped  $\text{Al}_2\text{O}_3$  and consider how these corrections influence the equilibrium concentrations of the defects.

The temperature correction to the chemical potential of a precursor is given by the equation [25, 26]

$$\Delta\mu(T, p_0) = \Delta H(T, p_0) - \Delta H(0, p_0) - TS(T, p_0), \quad (28)$$

where  $\Delta H(T, p_0)$  is the difference of enthalpy of the precursor at temperature  $T$  and at the reference temperature  $T_r = 298.15$  K, and  $S(T, p_0)$  is entropy at the standard pressure  $p_0 = 0.1$  MPa. The quantities  $\Delta H(0, p_0)$ ,  $\Delta H(T, p_0)$  and  $S(T, p_0)$  can be taken from the thermo-

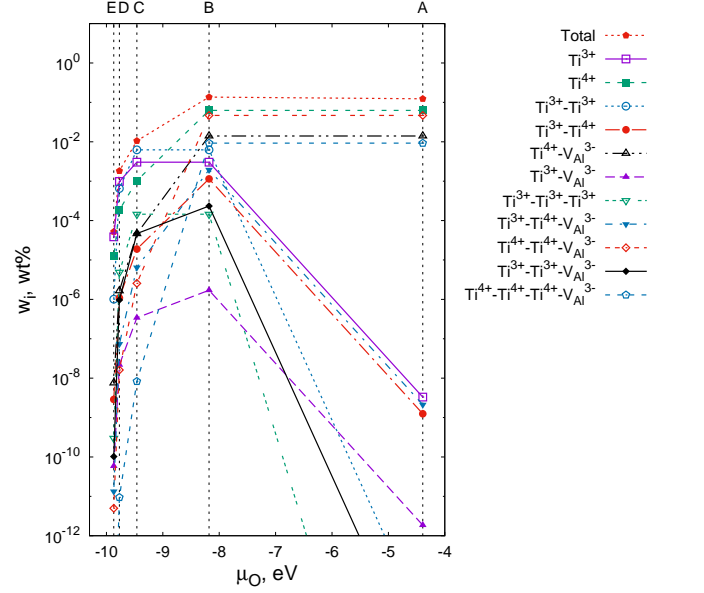


FIG. 4. Thermodynamically equilibrium total concentration of Ti in percent by mass and its distribution between defect species at the equilibrium points A - E at the temperature  $T = 1600$  K. Lines are guides to the eye.

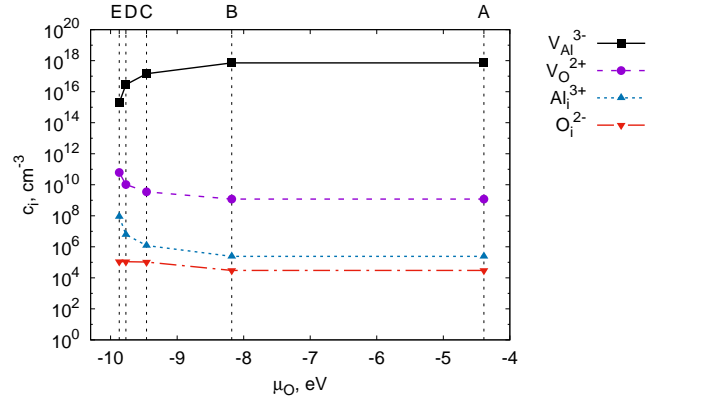


FIG. 5. Thermodynamically equilibrium concentrations of native defects at the temperature  $T = 1600$  K.

chemical tables [27]. The obtained  $\Delta\mu$  at  $T = 1600$  K are given in Table V.

Using the data of Tables II and V we plot the Al-Ti-O phase diagram Fig. 6 that accounts the temperature corrections to the formation energies (2) at  $T = 1600$  K. The equilibrium points A, B and C in Fig. 6 are

TABLE V. Temperature correction to the chemical potentials of precursors per formula unit (in eV) at  $T = 1600$  K.

Precursor	Al	Ti	$\text{Al}_2\text{O}_3$	$\text{TiO}_2$	$\text{Ti}_2\text{O}_3$	TiO	$\text{O}_2$
$\Delta\mu(1600, p_0)$	-0.901	-0.883	-2.278	-1.713	-3.020	-1.232	-3.770

the same as in the diagram Fig. 1. The phases  $\text{TiAl}_n$  ( $n = 1, 2, 3$ ) are not included in the diagram Fig. 6 due to lack of thermochemical data for these compounds in [27]. The points  $D$ ,  $E$  and  $F$  are replaced with the point  $F'$  that corresponds to the equilibrium between  $\text{Al}_2\text{O}_3$ ,  $\text{TiO}$  and the liquid phase of  $\text{Al}$ . Taking into account the correction (28) we obtain the temperature corrections to the chemical potentials of atoms  $\Delta\mu_X(T)$  ( $X = \text{Al}, \text{Ti}, \text{O}$ ) at the equilibrium points  $A$ ,  $B$ ,  $C$  and  $F'$ .

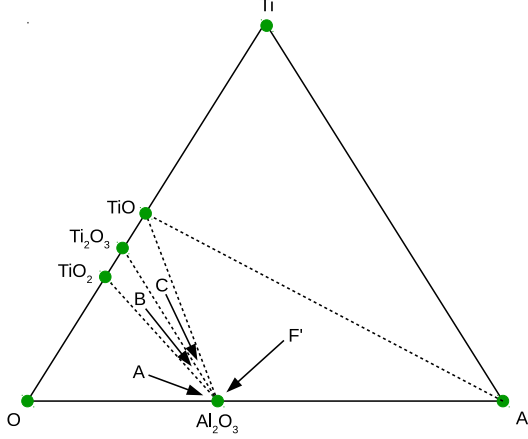


FIG. 6. Phase diagram of the Al-Ti-O ternary system at  $T = 1600$  K obtained in the approach that combines DFT and classical thermodynamics.

The defect formation energy (1) contains the difference of energies of a defect and the perfect supercell  $E_{\text{def-perf}} = E_{\text{def}} - E_{\text{perf}}$ . The DFT approach yields this difference at  $T = 0$  K. In the combined approach one should account not only the temperature corrections to the chemical potentials of atoms but a temperature correction to the difference  $E_{\text{def-perf}}$ , as well. For the supercell with substitutional Ti atoms we evaluate this correction as the difference of  $\Delta\mu_{\text{Ti}}(T)$  in  $\text{Ti}_2\text{O}_3$  and  $\Delta\mu_{\text{Al}}(T)$  in  $\text{Al}_2\text{O}_3$ . These compounds have the same crystal structure and the difference in  $\Delta H$  and  $S$  is caused in the main part by the replacement of Ti with Al. It yields  $\Delta E_{\text{def-perf}} = -0.371$  eV at  $T = 1600$  K per one substitutional Ti atom. For the supercell with one Al vacancy the temperature correction can be evaluated as  $\Delta\mu(T, p_0)$  for Ti crystal (see Table V) minus  $\Delta E_{\text{def-perf}}$  for the supercell with one substitutional Ti ion (we use Ti crystal as a reference compound since Al is in a liquid phase at  $T = 1600$  K). It yields  $\Delta E_{\text{def-perf}} = -0.513$  eV at  $T = 1600$  K per one vacancy. Taking into account the temperature corrections  $\Delta\mu_{\text{Al}}$ ,  $\Delta\mu_{\text{Ti}}$ ,  $\Delta\mu_{\text{O}}$  and  $\Delta E_{\text{def-perf}}$  in Eq. (1) we calculate the defect formation energies at  $T = 1600$  K. Using these energies we obtain from Eqs. (10)-(13) the concentrations of the defects. The result is presented in Fig. 7. One can see that the concentrations obtained from the formation energies in which the temperature corrections are neglected (Fig. 4) and from the formation energies that account the

temperature corrections (Fig. 7) demonstrate basically the same behavior under variation of the oxygen chemical potential. There are some minor differences, namely, in the oxidized conditions the calculations that account the temperature corrections yield higher concentrations of  $\text{Ti}^{3+}$  ions in comparison with the calculations where such corrections are neglected. In the reduces conditions the concentration of  $\text{Ti}^{4+}$  ions is underestimated if the temperature corrections are neglected. In the intermediate conditions the temperature corrections to the defect formation energies are rather small and result only in unessential changes of equilibrium concentrations of the defects.

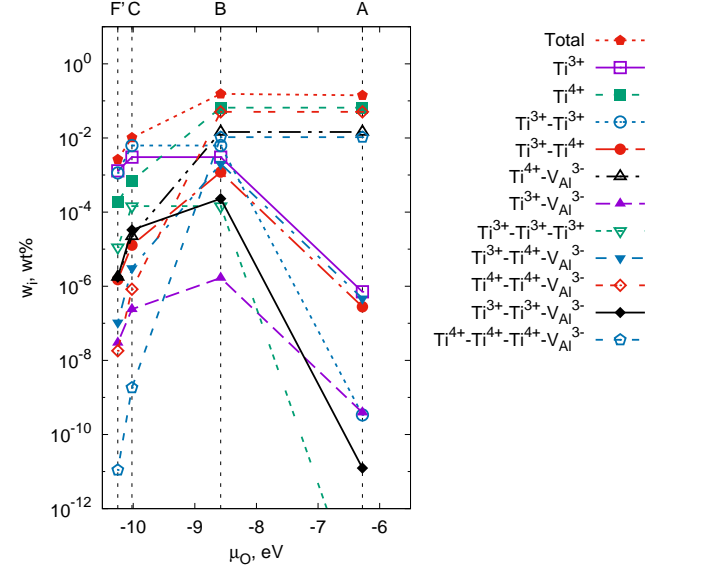


FIG. 7. Thermodynamically equilibrium total and partial concentrations of Ti at the temperature  $T = 1600$  K obtained in the approach that combines DFT and classical thermodynamics.

### C. Equilibrium concentration of defects in Ti-deficient conditions

Let us now consider a situation where the total concentration of Ti is less than the equilibrium one. To obtain partial concentrations of defects one should minimize the free energy (7) with the additional constraint

$$\sum_i k_i n_i = n_{\text{Ti}}, \quad (29)$$

where  $n_{\text{Ti}}$  is the total number of Ti atoms in the crystals. In this case we exclude  $n_3$  (the number of  $\text{Ti}^{3+}$ ) and  $n_V$  from the free energy (7) and find the extremum condition for the free energy (7) with respect to  $n_4$  and all other  $n_i$ . We arrive at the equations

$$E_4 - E_3 + \frac{1}{3}E_V$$



$$+k_B T \left( \ln \tilde{n}_4 + \frac{1}{3} \ln \tilde{n}_V - \ln \tilde{n}_3 \right) = 0, \quad (30)$$

$$k_B T \left( \frac{q_i}{3} \ln \tilde{n}_V + \ln \tilde{n}_i - k_i \ln \tilde{n}_3 \right) = 0. \quad (31)$$

From Eqs. (30) and (31) we obtain the following relations for the concentrations

$$\tilde{n}_4 \tilde{n}_V = \tilde{n}_3^3 \exp \left( \frac{3E_3 - 4\tilde{E}_4}{k_B T} \right), \quad (32)$$

$$\tilde{n}_i = \tilde{n}_4^{q_i} \tilde{n}_3^{k_i - q_i} \exp \left( \frac{(k_i - q_i)E_3 - E_i + q_i E_4}{k_B T} \right). \quad (33)$$

Using Eqs. (32) and (33) we find that the relation between the concentrations of isolated and complex defects is exactly the same as above (Eq. (15)). It is remarkable that the restriction (29) does not change this relation. Substituting the relation (15) into Eqs. (10), (29) and solving them together with Eq. (32) we obtain  $\tilde{n}_3$ ,  $\tilde{n}_4$  and  $\tilde{n}_V$ .

Let us restrict ourselves with seven defect species: three isolated defects ( $\text{Ti}^{3+}$ ,  $\text{Ti}^{4+}$  and  $V_{\text{Al}}^{3-}$ ) and four complex defects ( $\text{Ti}^{3+} - \text{Ti}^{3+}$  pairs,  $\text{Ti}^{4+} - V_{\text{Al}}^{3-}$  pairs,  $\text{Ti}^{4+} - V_{\text{Al}}^{3-} - \text{Ti}^{4+}$  triples and  $\text{Ti}^{4+} - \text{Ti}^{4+} - \text{Ti}^{4+} - V_{\text{Al}}^{3-}$  quadruples). Within this simplification Eqs. (10) and (29) are reduced to the following ones

$$\tilde{n}_4 - 3\tilde{n}_V - 8\tilde{n}_4\tilde{n}_V e^{\frac{E_{4V}^{(b)}}{k_B T}} - 6\tilde{n}_4^2\tilde{n}_V e^{\frac{E_{4V4}^{(b)}}{k_B T}} = 0, \quad (34)$$

$$\begin{aligned} \tilde{n}_3 + \tilde{n}_4 + 4\tilde{n}_3^2 e^{\frac{E_{33}^{(b)}}{k_B T}} + 4\tilde{n}_4\tilde{n}_V e^{\frac{E_{4V}^{(b)}}{k_B T}} \\ + 12\tilde{n}_4^2\tilde{n}_V e^{\frac{E_{4V4}^{(b)}}{k_B T}} + 12\tilde{n}_4^3\tilde{n}_V e^{\frac{E_{4V4}^{(b)}}{k_B T}} = \frac{n_{\text{Ti}}}{N_{\text{Al}}}, \end{aligned} \quad (35)$$

where  $E_{33}^{(b)}$  is the binding energy of  $\text{Ti}^{3+} - \text{Ti}^{3+}$  pairs. Solving the system (32), (34), (35) we obtain the concentrations  $\tilde{n}_i$ . In Fig. 8 the distribution of Ti (in wt%) between different defect species at the points *B* and *C* of the phase diagram is shown. Since in the intermediate conditions the temperature corrections to the defect formation energies are small we neglect them in the calculations. One can see that the deficit of Ti results in two effects. First, the relative fraction of complex defects decreases. Second, the ratio of isolated  $\text{Ti}^{4+}$  ions to  $\text{Ti}^{3+}$  ions increases.

### D. Ti impurity levels in the band structure

The presence of Ti in  $\alpha\text{-Al}_2\text{O}_3$  results in an appearance of additional levels in the band gap. To obtain these levels we compute the band structures of  $\alpha\text{-Al}_2\text{O}_3$  with one defect in the supercell. A 120-atom supercell with one, two and three Ti atoms contains 1.9 wt%, 3.8 wt% and 5.7 wt% of Ti, correspondingly. It is much larger than the equilibrium concentration of Ti calculated above, but

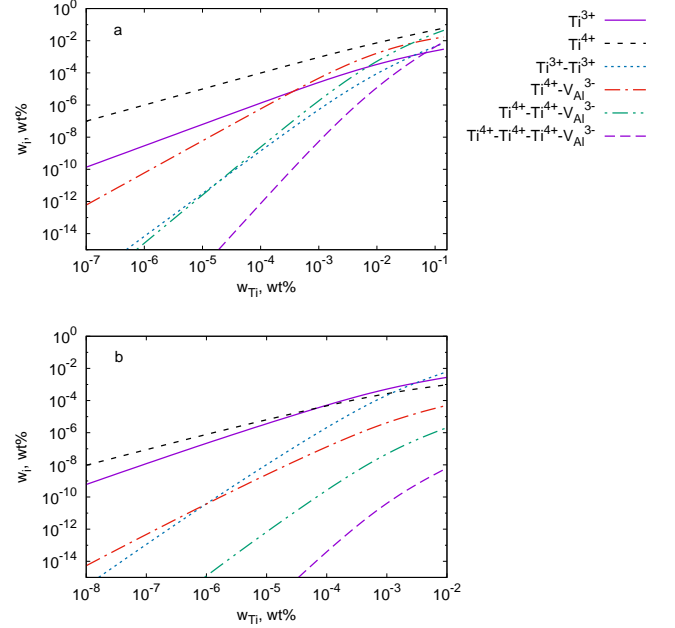


FIG. 8. Contributions of different defect species into the total Ti concentration  $w_{\text{Ti}}$  in the Ti-deficient conditions at the equilibrium points B (a) and C (b) of the phase diagram.

since our band structure calculations yield very narrow impurity bands (see below) such calculations describe adequately impurity levels at low Ti concentration.

In Fig 9a the calculated band structure of the perfect  $\alpha\text{-Al}_2\text{O}_3$  is shown. The Brillouin zone corresponds to the 120-atom supercell. The calculated band gap is  $E_g = 4.91$  eV. Underestimation of  $E_g$  (experimental value is 8.7 eV) is a known band gap prediction problem of the standard DFT methods based on the PBE functional [28] as well as on the local-density approximation (see, for instance [29]). In [29] it was proposed to use the modified Becke-Johnson (MBJ) potential for accurate calculations of the band gap. The MBJ potential is a modified version of the original Becke-Johnson (BJ) exchange potential [30]. The MBJ potential contains the Becke-Roussel (BR) potential [31] instead of the Slater exchange potential. The BR potential and the MBJ potentials are quasilocal ones: they are determined by the electron density and its first and second spatial derivatives. In [32] the MBJ potential was employed to study the structural, electronic, and optical properties of doped  $\alpha\text{-Al}_2\text{O}_3$ . In [32] the band gap of pure  $\alpha\text{-Al}_2\text{O}_3$  was calculated by the full potential linear augmented plane wave method with the PBE and MBJ potentials. The PBE calculations yields  $E_g = 6.5$  eV, but the result of MBJ calculations is very close ( $E_g = 8.5$  eV) to the experimental value. The authors of [32] considered impurity levels of yttrium, scandium, zirconium and niobium doped  $\alpha\text{-Al}_2\text{O}_3$  crystals. They found that the same impurity induced peaks in the density of states appear in the PBE and mBJ calculations. These peaks have the same or-

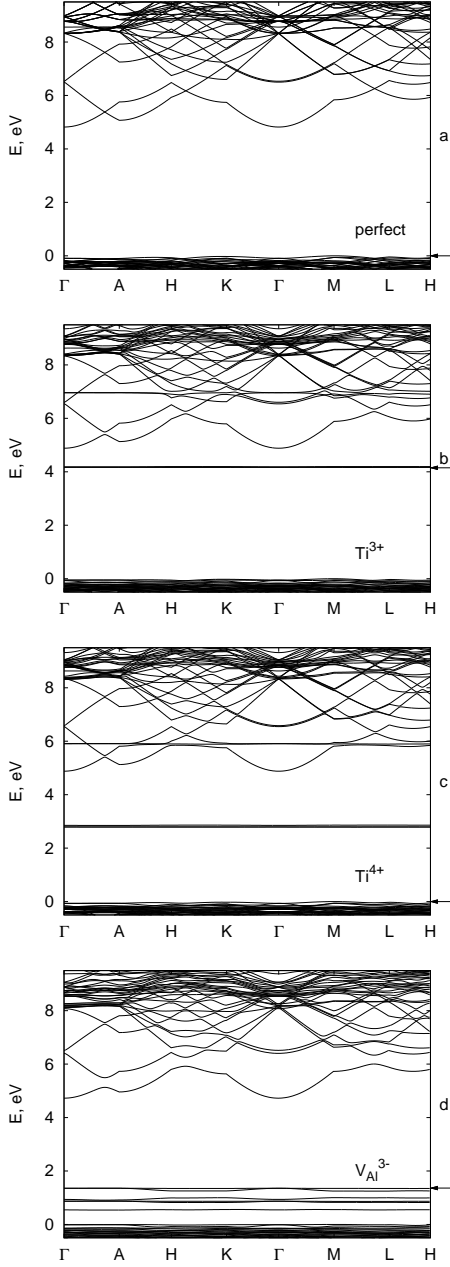


FIG. 9. Band structure of the perfect  $\alpha - \text{Al}_2\text{O}_3$  (a) and  $\alpha - \text{Al}_2\text{O}_3$  with one isolated defect (b,c,d) per supercell. The valence band maximum is set at 0 eV, and the arrow indicates the position of the highest occupied level.

bit decomposition and the relative positions within the gap, although their width and absolute positions are sensitive to the potential used. The authors of [32] have concluded that the PBE and mBJ calculations of impurity levels produce qualitatively similar results, which can be interpreted in the same way. Basing on this conclusion we expect that the method implemented in SIESTA code allows to analyze adequately impurity levels in Ti-doped  $\alpha - \text{Al}_2\text{O}_3$  with complex defects.

In Fig. 9b and 9c we present the calculated band struc-

tures of  $\alpha - \text{Al}_2\text{O}_3$  with one  $\text{Ti}^{3+}$  and one  $\text{Ti}^{4+}$  per supercell, correspondingly. One can see that isolated Ti defects reveal itself in an appearance of two impurity levels which correspond to  $t_{2g}$  (lower) and  $e_g$  (higher) states. For  $\text{Ti}^{4+}$  the lower level is much closer to the valence band maximum (VBM) than for  $\text{Ti}^{3+}$  (2.86 eV against 4.22 eV). Similar results were obtained in [14]. The energy separation between the lower and the higher level is larger for  $\text{Ti}^{4+}$  than for  $\text{Ti}^{3+}$  (3.11 eV against 2.79 eV). The additional splitting of  $t_{2g}$  level is small (0.01 eV for  $\text{Ti}^{3+}$  and 0.06 eV for  $\text{Ti}^{4+}$ ). Our calculations overestimate the separation between  $e_g$  and  $t_g$  levels in comparison with experimental data [33] (2.37 eV). The positions and separations of impurity levels shown in Fig. 7b are similar to ones obtained in [34, 35] for larger Ti concentration. Isolated Al vacancies (Fig. 9d) reveal itself in the appearance of oxygen levels inside the band gap near the VBM.

In Fig. 10 the band structure of  $\alpha - \text{Al}_2\text{O}_3$  with defect pairs is presented. The a,b and c panels of Fig. 10 correspond to  $\text{Ti}^{3+} - \text{Ti}^{3+}$ ,  $\text{Ti}^{3+} - \text{Ti}^{4+}$  and  $\text{Ti}^{4+} - \text{V}_{\text{Al}}^{3-}$  pairs, respectively. We consider the configurations with the lowest formation energy. One Ti atom or Al vacancy is located at the central site (Fig. 2) and another Ti atom, at the apex site belonging to the tetrahedron base. One can see from the comparison of Figs. 9 and 10 that the formation of defect pairs results in splitting of Ti impurity levels.

In the presence of  $\text{Ti}^{3+} - \text{Ti}^{3+}$  pairs (Fig. 10a) the energy distance between the lowest occupied level and the 6-th level is 2.43 eV (510 nm). It is larger than one obtained in [15]. We connect this discrepancy with the following. In [15] the band structure was calculated for the  $\text{Ti}^{3+}\text{Ti}^{3+}$  pair oriented along the [0001] axis while another orientation of that pair was implied in our calculations. The presence of  $\text{Ti}^{3+} - \text{Ti}^{4+}$  pairs (Fig. 10b) results in the appearance of a number of empty impurity levels, one of which is located at around 1.37 eV (900 nm) to the occupied level. This energy distance can be related to the experimentally observed infrared absorption peak at 800 nm.

In Fig. 11 the band structure of  $\alpha - \text{Al}_2\text{O}_3$  with triple and quadruple defects is displayed. The defects are formed by an Al vacancy at the central site (Fig. 2) and two or three Ti ions located at apex sites of the tetrahedron base. It corresponds to the lowest formation energy configurations. Comparing Fig. 10b and 11a we conclude that the binding of Al vacancies with  $\text{Ti}^{3+} - \text{Ti}^{4+}$  pairs results in a red shift of the infrared absorption peak. Our calculations yield the shift  $\Delta E = 0.43$  eV. This shift can result in an increase of FoM of Ti:sapphire lasers.

One can see from Figs. 9c, 10c, 11b and 11c that the lowest  $\text{Ti}^{4+}$  level lifts up relative VBM under the binding of  $\text{Ti}^{4+}$  with  $\text{V}_{\text{Al}}^{3-}$ . The additional higher levels also appear under such a binding. The latter may influence only insignificantly on characteristics of Ti:sapphire lasers.

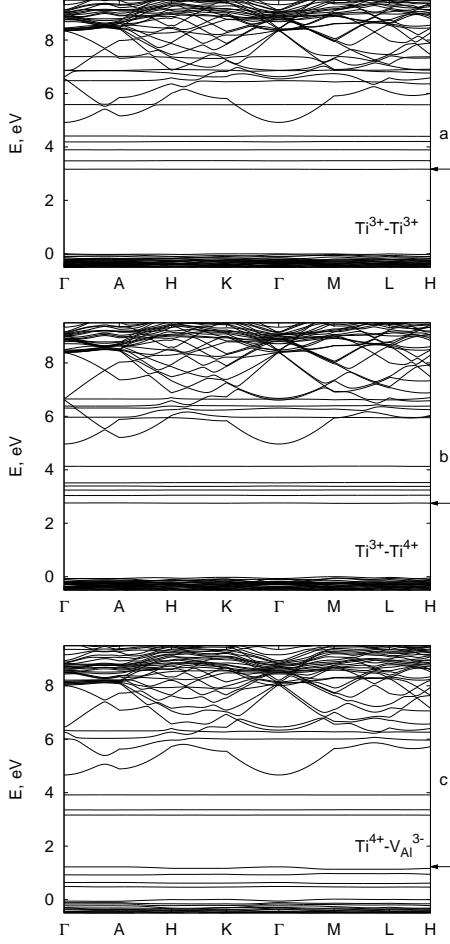


FIG. 10. Band structure of  $\alpha - \text{Al}_2\text{O}_3$  with one defect pair per supercell.

#### IV. CONCLUSION

In conclusion we have found by the first-principles calculations that Ti-doped  $\alpha\text{-Al}_2\text{O}_3$  contains a large fraction of complex defects (pair, triples, quadruples) formed by  $\text{Ti}^{3+}$  and  $\text{Ti}^{4+}$  substitutional ions and Al vacancies  $V_{\text{Al}}^{3-}$ . Partial concentrations of these defects depend on the oxygen chemical potential. A significant fraction of complex defects formed by one, two or three  $\text{Ti}^{4+}$  ions and one  $V_{\text{Al}}^{3-}$  vacancy emerges in the oxidized and intermediate conditions, while a large fraction of  $\text{Ti}^{3+}$  pairs appears in the reduced conditions. Our calculations yield a rather small fraction of  $\text{Ti}^{3+} - \text{Ti}^{4+}$  pairs. The concentration of such pairs reaches the maximum in the intermediate conditions.  $\text{Ti}^{3+} - \text{Ti}^{4+}$  pairs demonstrate a tendency to bind in triples with  $V_{\text{Al}}^{3-}$  vacancies.

Ti-deficient conditions are also analyzed. It is shown that the deficit of Ti leads to a decrease in the complex defect fraction and to an increase in the isolated defect fraction with the shift of the balance between  $\text{Ti}^{3+}$  and  $\text{Ti}^{4+}$  toward the ions with larger valence.

A universal relation between the concentrations of iso-

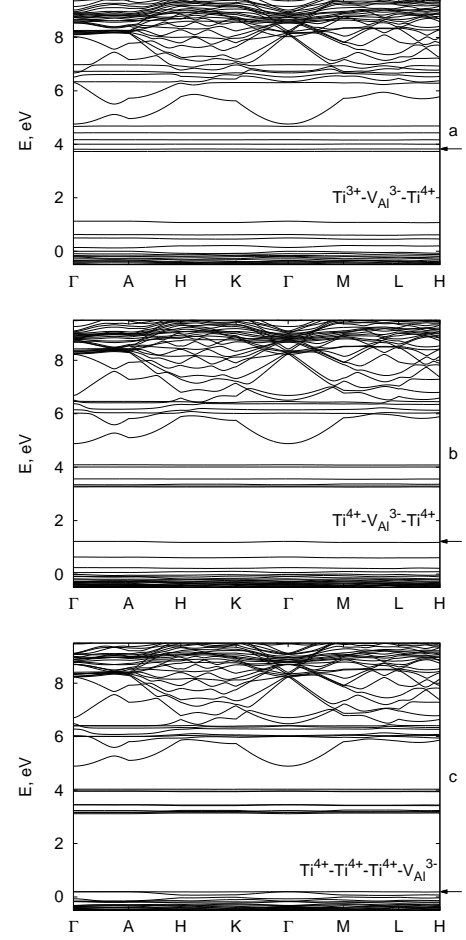


FIG. 11. Band structure of  $\alpha\text{-Al}_2\text{O}_3$  with one complex (triple or quadruple) defect per supercell.

lated and complex defects valid for any total Ti concentration is obtained.

The influence of defect clustering on impurity levels inside the band gap is considered. It is found that the binding of Al vacancies with  $\text{Ti}^{3+} - \text{Ti}^{4+}$  pairs results in a red shift of the infrared absorption peak. At the same time the binding of Al vacancies with  $\text{Ti}^{4+}$  ions may influence only insignificantly the laser characteristics of Ti:sapphire.

#### ACKNOWLEDGMENTS

This work was performed using computational facilities of the Joint computational cluster of State Scientific Institution "Institute for Single Crystals" and Institute for Scintillation Materials of National Academy of Sciences of Ukraine incorporated into Ukrainian National Grid.

- 
- [1] Marvin J. Weber, *Handbook of Lasers* (CRC Press LLC, Boca Raton, USA, 2001).
- [2] P. Moulton, *Optics News* **8**(6), 9 (1982).
- [3] P. Lacovara, L. Esterowitz and M. Kokta, *IEEE Journal of Quantum Electronics* **21**, 1614 (1985).
- [4] P. Moulton, *Journal of the Optical Society of America B* **3**, 125 (1986).
- [5] A. Sanchez, A. J. Strauss, R. L. Aggarwal and R. E. Fahey, *IEEE Journal of Quantum Electronics* **24**, 995 (1988).
- [6] W. R. Rapoport and C. P. Khattak, *Applied Optics* **27**, 2677 (1988).
- [7] F. X. Zha, J. H. Zhang and S. D. Xia, *J. Phys.: Condens. Matter* **6**, 6497 (1994).
- [8] R. Uecker, D. Klimm, S. Ganschow, P. Reiche, R. Bertram, M. Rossberg and R. Fornari, *Proc. SPIE* **5990**, *Optically Based Materials and Optically Based Biological and Chemical Sensing for Defence II*, 599006 (2005).
- [9] S.V. Nizhankovskii, N.S. Sidelnikova and V.V. Baranov, *Physics of the Solid State* **57**, 781 (2015).
- [10] K. Matsunaga, T. Tanaka, T. Yamamoto and Y. Ikuhara, *Phys. Rev. B* **68**, 085110 (2003).
- [11] N. D. M. Hine, K. Frensch, W. M. C. Foulkes and M. W. Finnis, *Phys. Rev. B* **79**, 024112 (2009).
- [12] M. Ghamnia, C. Jardin and M. Bouslama, *Journal of Electron Spectroscopy and Related Phenomena* **133**, 55 (2003).
- [13] X. Xiang, G. Zhang, X. Wang, T. Tang and Y. Shi, *Phys. Chem. Chem. Phys.* **17**, 29134 (2015).
- [14] K. Matsunaga, A. Nakamura, T. Yamamoto and Y. Ikuhara, *Phys. Rev. B* **68**, 214102 (2003).
- [15] K. Matsunaga, T. Mizoguchi, A. Nakamura, T. Yamamoto and Y. Ikuhara, *Appl. Phys. Lett.* **84**, 4795 (2004).
- [16] J. M. Soler, E. Artacho, J. D. Gale, A. Garcia, J. Junquera, P. Ordejon and D. Sanchez-Portal, *J. Phys.: Condens. Matter* **14**, 2745 (2002).
- [17] S. B. Zhang and J. E. Northrup, *Phys. Rev. Lett.* **67**, 2339 (1991).
- [18] W. B. Pearson, *A Handbook of Lattice Spacings and Structures of Metals and Alloys* (Pergamon Press, New-York, 1958).
- [19] H. d'Amour, D. Schiferl, W. Denner, H. Schulz and W. B. Holzapfel, *Journal of Applied Physics* **49**, 4411 (1978).
- [20] S. C. Abrahams and J. L. Bernstein, *J. Chem. Phys.* **55**, 3206 (1971).
- [21] M. G. Vincent, K. Yvon, A. Gruttner and J. Ashkenazi, *Acta Cryst.* **A36**, 803 (1980).
- [22] D. Watanabe, J. R. Castles, A. Jostsons, A. S. Malin, *Acta Cryst.* **23**, 307 (1967).
- [23] T. Novoselova, S. Malinov, W. Sha and A. Zhecheva, *Materials Science and Engineering A* **371**, 103 (2004).
- [24] J. Braun and M. Ellner, *Journal of Alloys and Compounds*, **309**, 118 (2000).
- [25] K. Reuter and M. Scheffler, *Phys. Rev. B* **65**, 035406 (2000).
- [26] K. Reuter and M. Scheffler, *Phys. Rev. Lett.* **90**, 046103 (2003).
- [27] M. W. Chase Jr., *JANAF Thermochemical Tables, 4th ed.*, (American Chemical Society and American Institute of Physics, New York, 1998).
- [28] J. M. Crowley, J. Tahir-Kheli and W. A. Goddard III, *J. Phys. Chem. Lett.* **7**, 1198 (2016).
- [29] F. Tran and P. Blaha, *Phys. Rev. Lett.* **102**, 226401 (2009).
- [30] A. D. Becke and E. R. Johnson, *J. Chem. Phys.* **124**, 221101 (2006).
- [31] A. D. Becke and M. R. Roussel, *Phys. Rev. B* **79**, 3761 (1989).
- [32] A. F. Lima, J. M. Dantas and M. V. Lalic, *J. Appl. Phys.* **112**, 093709 (2012).
- [33] S. Garcia-Revilla, F. Rodriguez, R. Valiente and M. Pollnau, *J. Phys.: Condens. Matter* **14**, 447 (2002).
- [34] J. Zhang, J. Ding and Y. Zhang, *Sol. St. Commun.* **149**, 1188 (2009).
- [35] M. G. Brik, *Physica B* in press (2017) (<https://doi.org/10.1016/j.physb.2017.02.032>).